Supplementary Information

Long-lifespan, flexible Zinc-ion secondary battery using paper-like cathode from single-atomic MnO_2 nanosheets

Yanan Wang[a], Zeyi Wu[a], Le Jiang[a], Wenchao Tian[a], Chenchen Zhang[b], Cailing Cai[a], Linfeng Hu[a]*

a. Department of Materials Science, Fudan University, Shanghai 200433, P. R. China

b. State Grid Anhui Electric Power Institute, Hefei, 230022, China

* E-mail: linfenghu@fudan.edu.cn.

Contents:

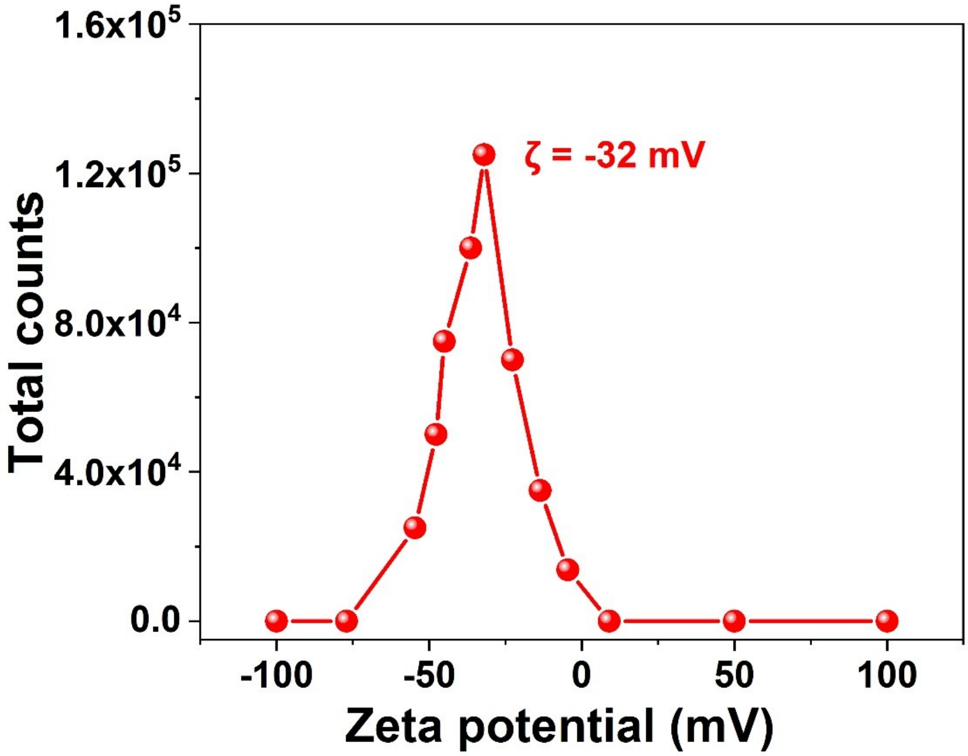

Figure S1 Zeta-potential curve of the as-exfoliated MnO_2 nanosheets dispersed in milli-Q water (40 mmol/L).

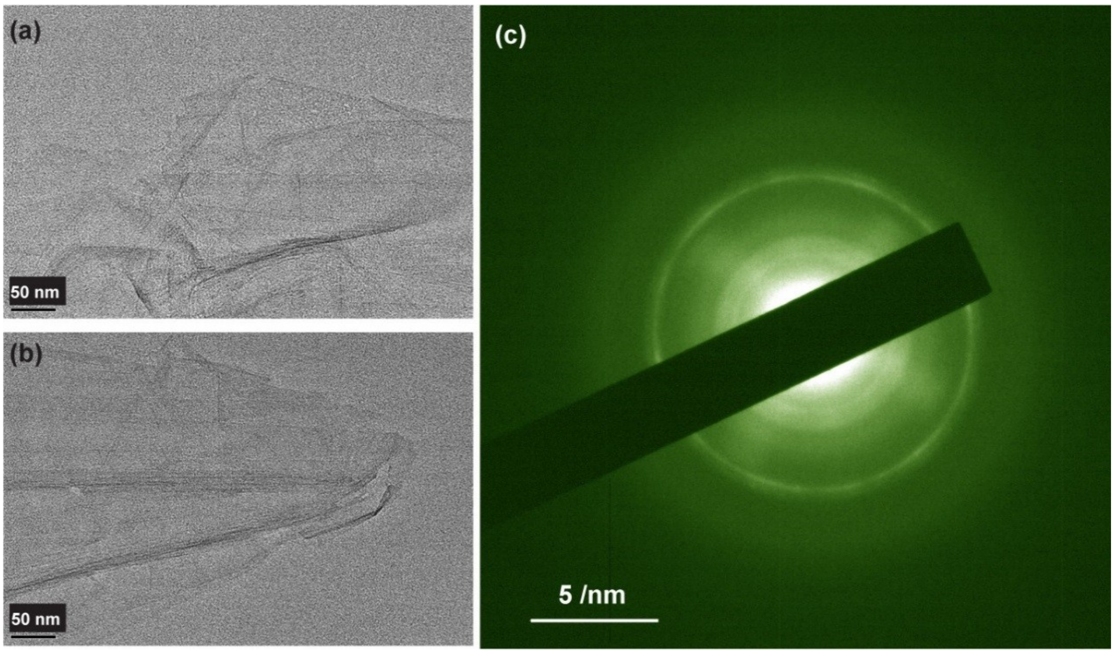

Figure S2 Typical TEM image and SAED pattern of MnO_2 single-layer nanosheets.

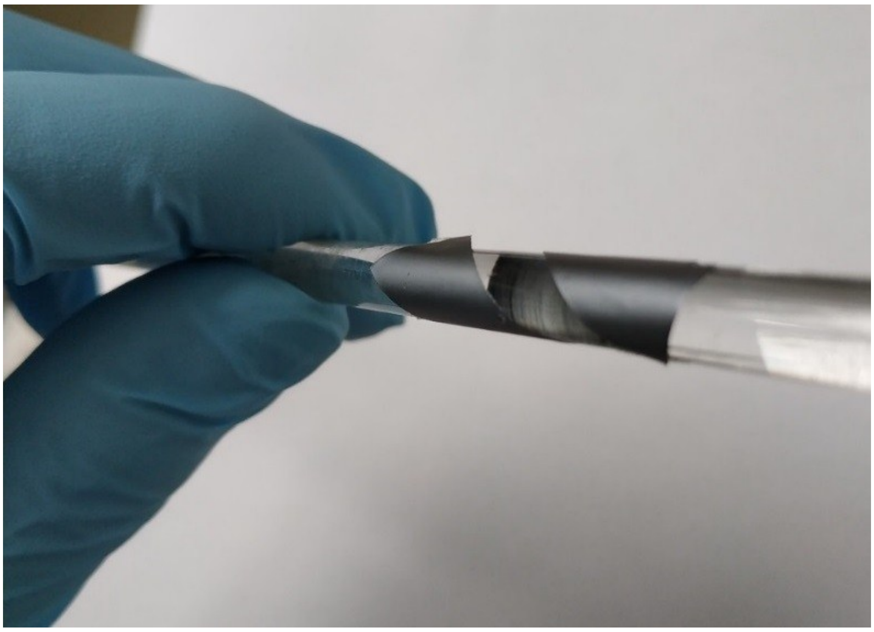

Figure S3. The MnO_2/MWCNTs hybrid membrane was coiled around a glass rod to illustrate the excellent flexibility.

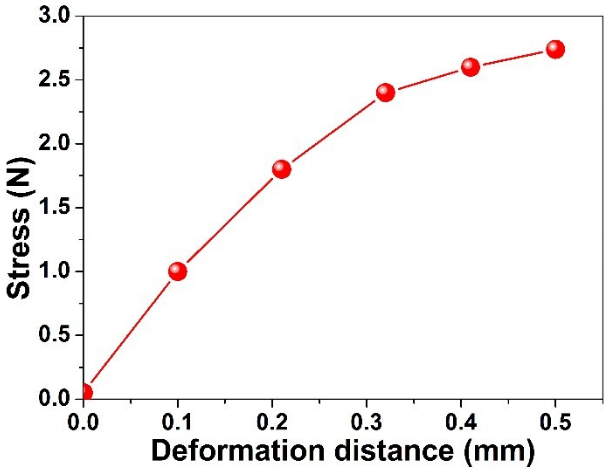

Figure S4 The tensile strength of the MnO_2/MWCNTs membrane. It has a maximum tensile force of 2.74N, an elongation at break of 1.6%.

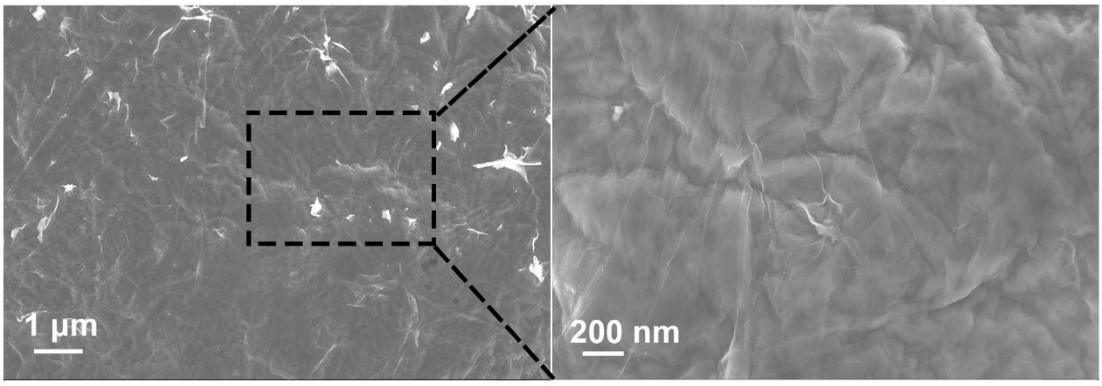

Figure S5 Top-view of the SEM images of the MnO_2/MWCNTs membrane to show the smooth surface morphology.

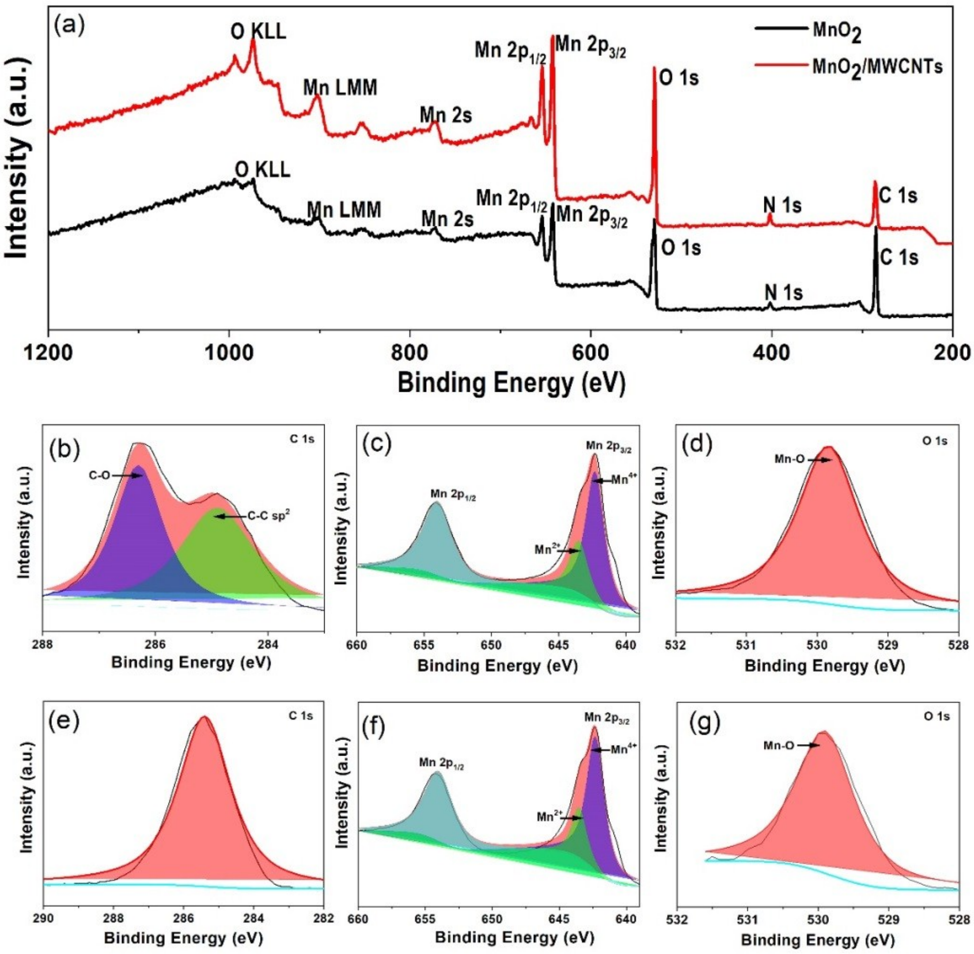

Figure S6 (a) Survey XPS spectrum of MnO_2 and MnO_2/MWCNTs. (b-d) C 1s, Mn 2p, and O1s XPS spectra of MnO_2 NS/MWCNTs membrane. (e-g) C 1s, Mn 2p, and O1s XPS spectra of MnO_2 membrane, respectively. As shown in high-resolution C 1s spectrum (**Figure S6**b) for MnO_2/MWCNTs, combining with the MWCNTs, two group of spin-orbit resolved peaks can be resolved corresponding to C-O (286.4 eV) and C-C (285.4 eV), while the C 1s state in MnO_2 membrane (**Figure S6**e) exists in the form of C-C (285.4 eV).[1,2] Mn 2p spectrum (**Figure S6**c, f) for MnO_2/MWCNTs and MnO_2 membranes, three group of spin-orbit resolved peaks can be resolved corresponding to Mn (2p1/2, 653.8 eV),[3] Mn^{2+} (2p3/2, 643.5 eV) and Mn^{4+} (2p3/2, 642.5 eV),[4,5] thus the Mn state in this hybrid exists in the form of Mn^{2+} and Mn^{4+}. The deconvoluted O 1s spectrum (**Figure S6**d, g), only one peak can be resolved corresponding to O-Mn (529.3 eV).[6]

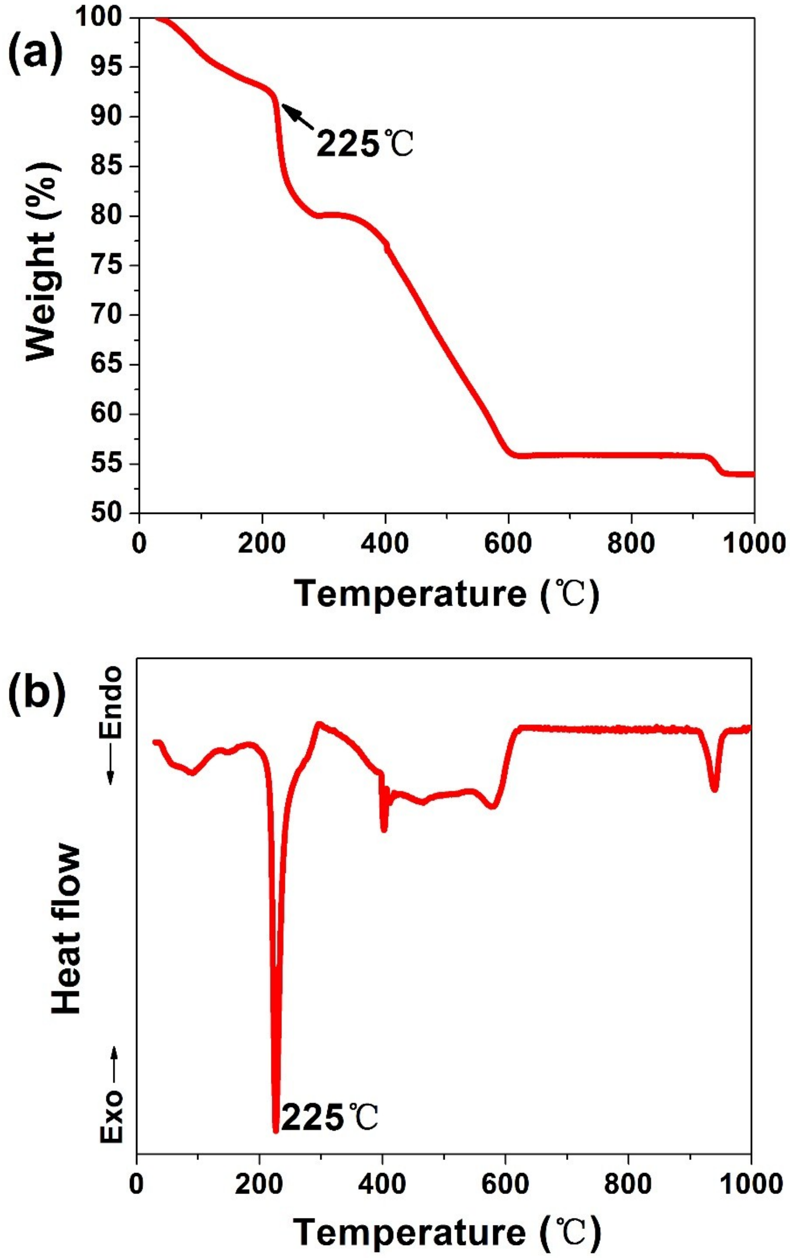

Figure S7 Thermal stability of the as-prepared MnO_2/MWCNTs hybrid membrane: (a) TGA and (b) DSC profiles.

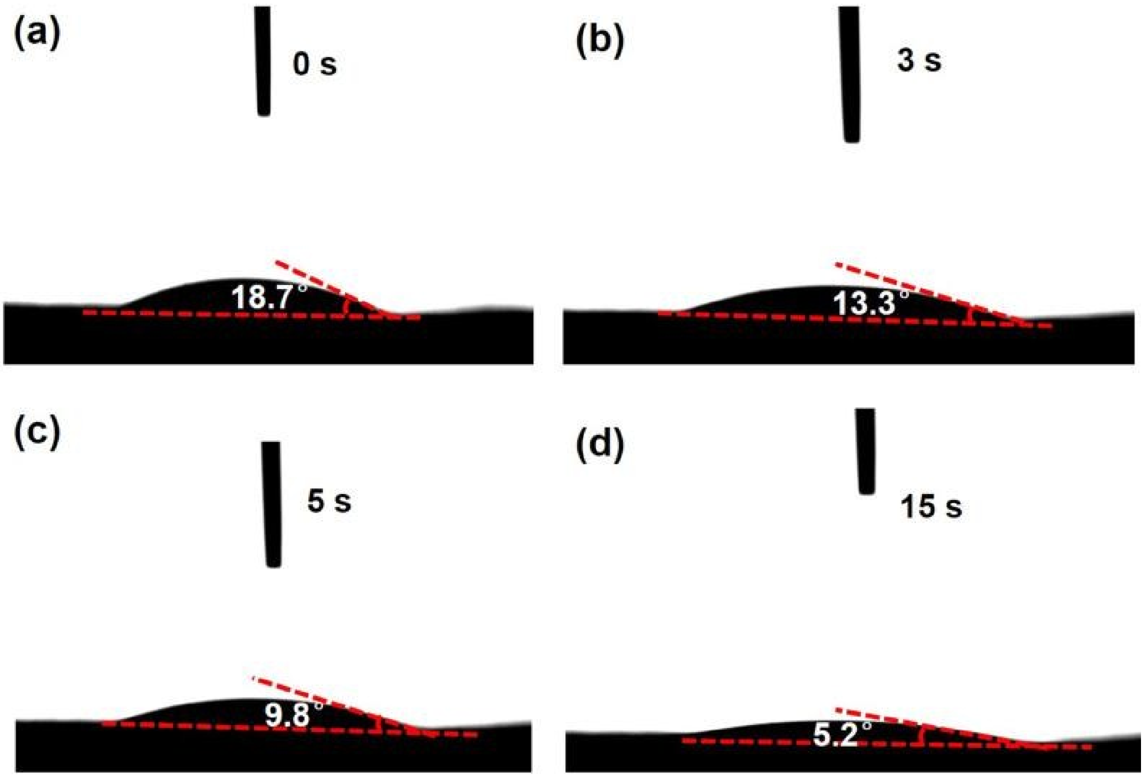

Figure S8 Contact angle evolution of MnO_2/MWCNTs membranes in aqueous electrolyte solution.

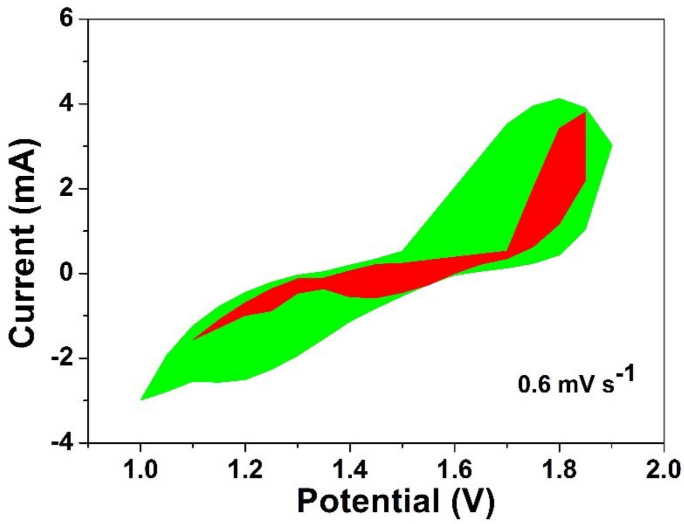

Figure S9 CV profile at 0.6 mV/s showing the capacitive contribution (red region) to the total current.

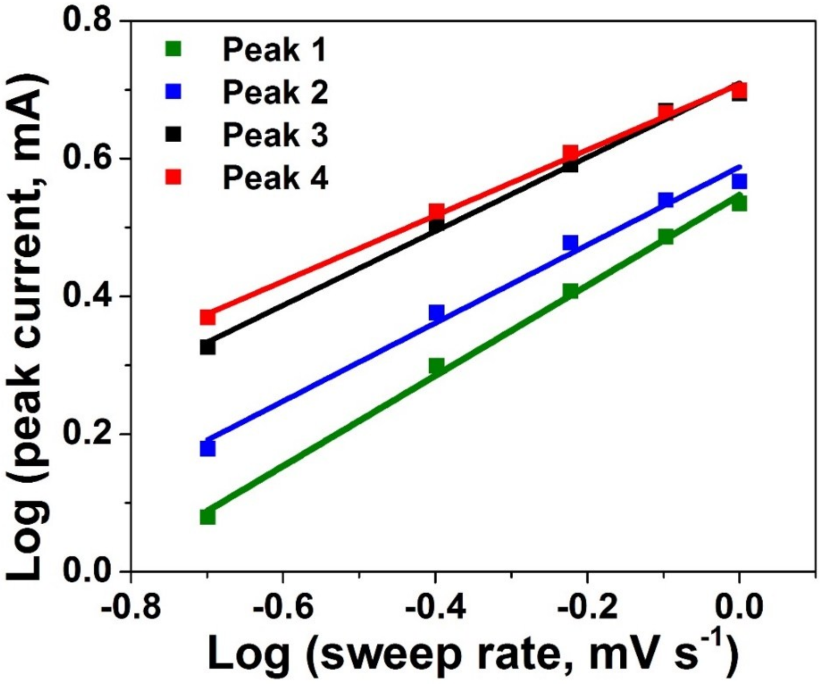

Figure S10 The logarithm dependence of peak current density and scan rate of the MnO_2/MWCNTs membrane -based ZIB in the *CV* test. In order to further explore the electrochemical kinetic of MnO_2/MWCNTs electrode, the logarithm dependence of peak current density *i* and various scan rates *v* in the *CV* test has been analyzed based on the following equation:[7]

$$i = a\, v^{b} \quad (1)$$

$$\log i = \log a + b \log v \quad (2)$$

Where parameters *a* and *b* are adjustable parameters, with *b* (range from 0.5 to 1.0) represents the slope of *log i* versus *log v* in Supplementary Fig. S8. It's obviously that the *b* value of 0.5 represents a diffusion-controlled insertion process, while the *b* value of 1.0 reflects a surface capacitive process.[8,9] With the linear plots of *log i* and *log v*, the *b* values of four redox peaks are calculated as 0.66 (peak 1), 0.57 (peak 2), 0.54 (peak 3), and 0.51 (peak 4), respectively. It indicates that the electrochemical kinetic of MnO_2/MWCNTs electrode is affected by diffusion-controlled process and capacitive effects, while the former plays the dominant role.

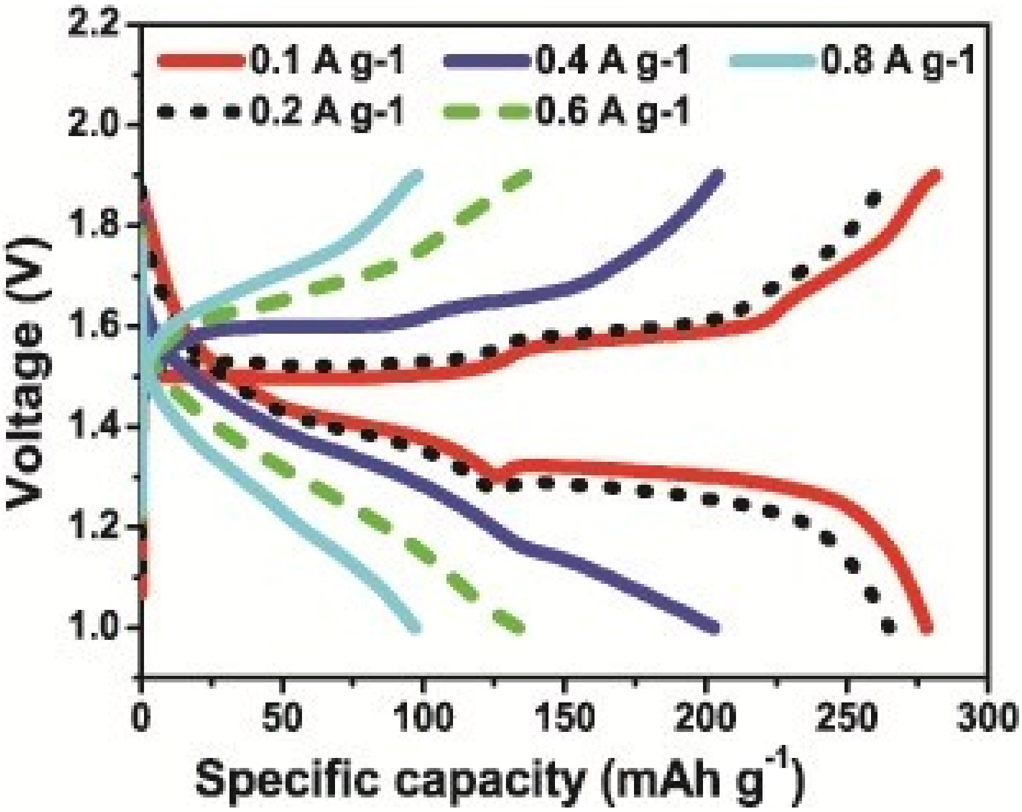

Figure S11 The galvanostatic charge/discharge curves of the MnO_2/MWCNTs membrane-based ZIBs at various current densities of 0.1, 0.2, 0.4, 0.6 and 0.8 A·g^{-1}, respectively.

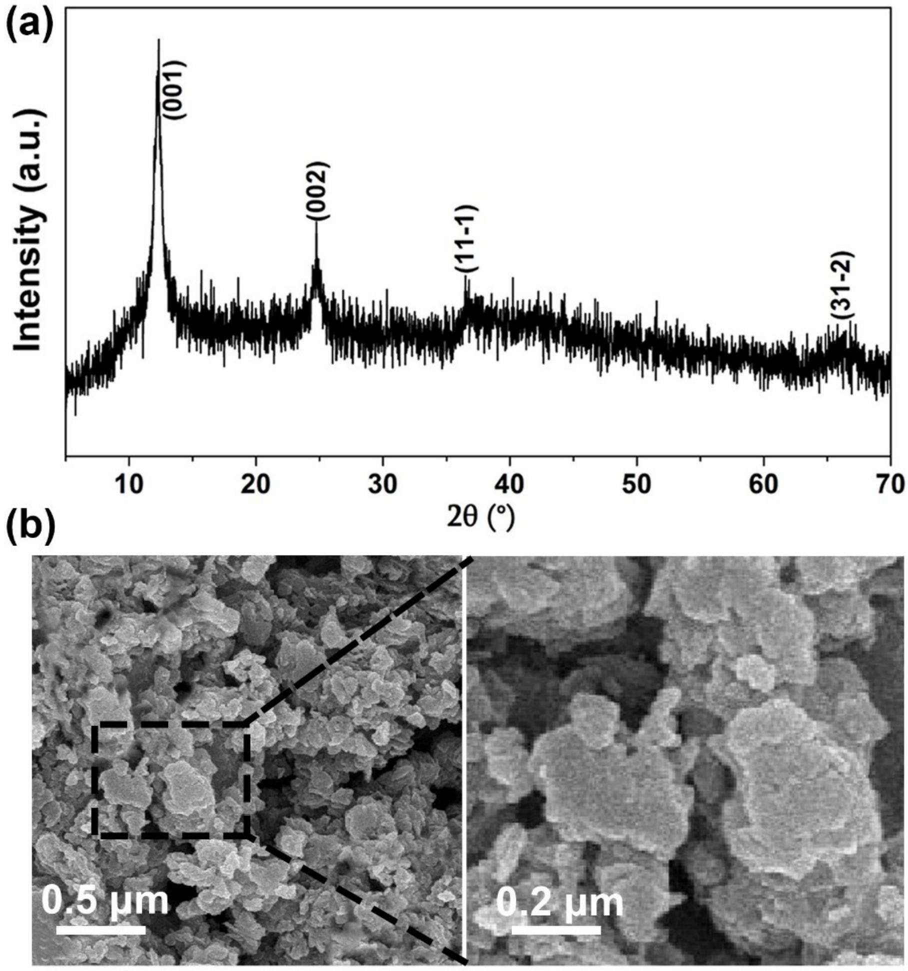

Figure S12 (a) XRD and (b) SEM of the δ-MnO_2 bulk prepared by the thermal decomposition of $KMnO_4$.

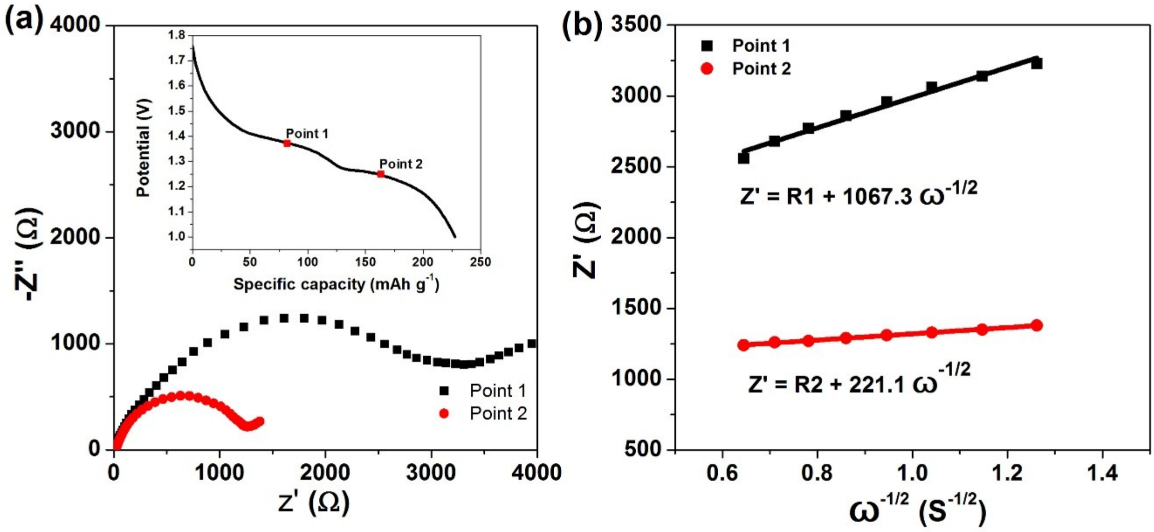

Figure S13 (a) Nyquist spectrum of MnO_2 bulk electrodes measured at the corresponding point on the discharge curve (inset) for Zn^{2+} diffusion coefficient analysis. (b) *Z' vs.* $\omega^{-1/2}$ plots in the low frequency region obtained from the electrochemical impedance spectroscopy measurements.

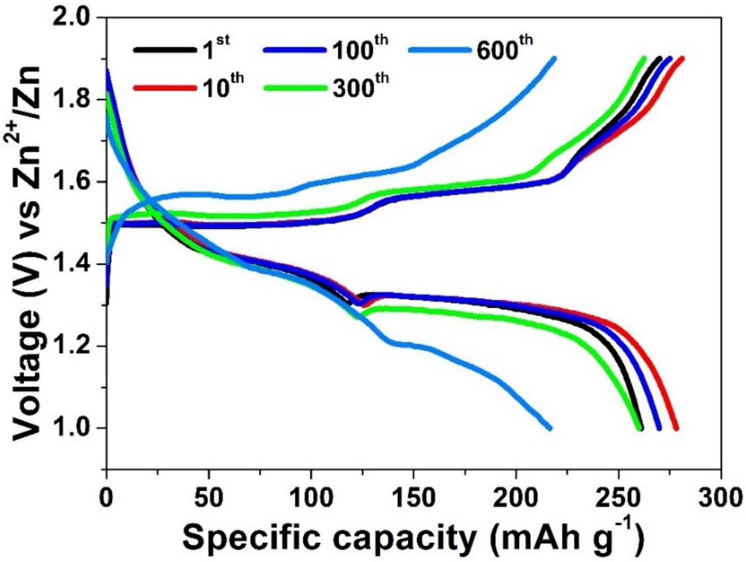

Figure S14 Galvanostatic charge/discharge curves of the MnO_2/MWCNTs membrane-based ZIB at the cycle number of 1st, 10th, 100th, 300th, and 600th, respectively.

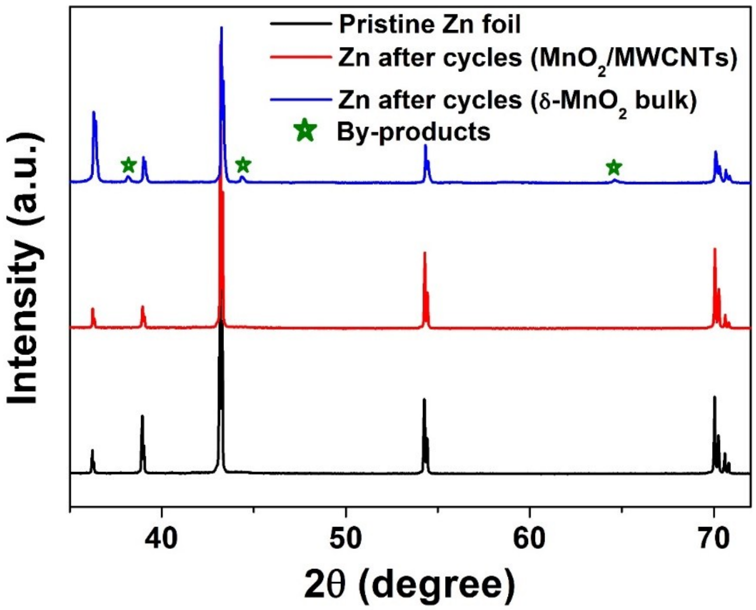

Figure S15 XRD of the pristine Zn foil anode and the Zn foil after 600 cycles disassembled from the ZIBs constructed from δ-MnO_2 bulk and the MnO_2/MWCNTs membrane, respectively.

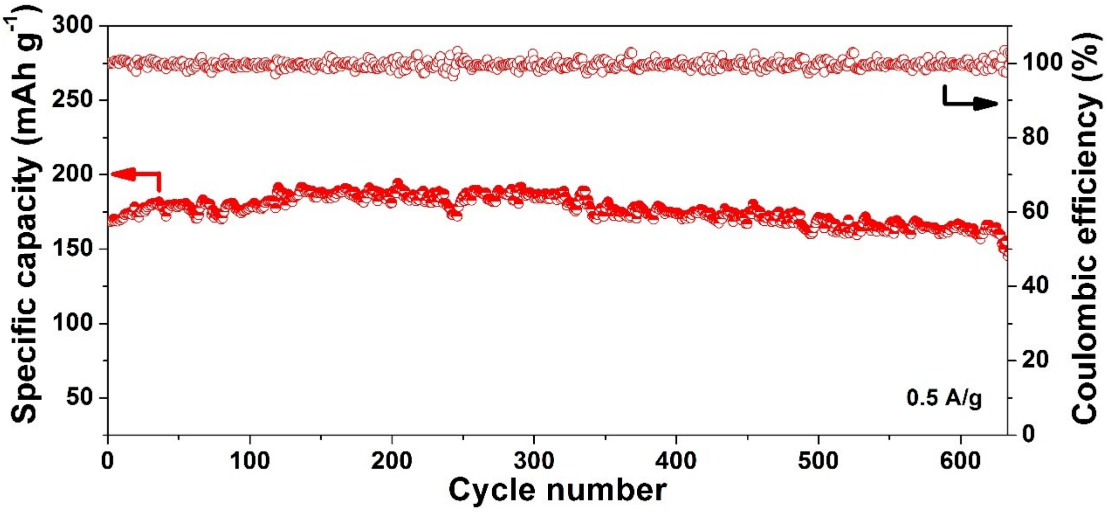

Figure S16 Cycle performance of the flexible ZIBs at 0.5 A/g.

Table S1. Comparison of specific capacity, cycle number and rate properties

Cathode material	electrolyte	Specific capacity (mAh g^{-1})	cycle number (rete A/g)	Rete properties
δ-MnO_2[10]	acetonitrile−$Zn(TFSI)_2$	123 (0.04 C)	125 (0.04C)	0.04-1 C
δ-MnO_2[11]	1 M $ZnSO_4$	252 (0.083 A/g)	100 (0.083 A/g)	0.083-1.67 A/g
$ZnMn_2O_4$[12]	3 M $Zn(CF_3SO_3)_2$	150 (0.5 A/g)	500	—
MnO_2@ZHS[13]	2 M $ZnSO_4$ + 0.24 M $MnSO_4$	155.4 (0.5 A/g)	1500 (0.5 A/g)	—
ε-MnO_2[14]	1 M $ZnSO_4$ + 1 M $MnSO_4$	221 (0.1 A/g)	500 (0.5 A/g)	0.1-2 A/g
MnO_2/CNT/PANI composites[15]	2 M $ZnSO_4$ + 0.5 M $MnSO_4$	310 (0.1 A/g)	340 (0.5 A /g)	0.1-5 A/g
MnO_2/rGO[7]	2 M $ZnSO_4$ + 0.1 M $MnSO_4$	332.2 (0.3 A/g)	500 (6A/g)	0.3-6 A/g
β-MnO_2 nanorods[16]	3 M $Zn(CF_3SO_3)_2$ + 0.1 M $Mn(CF_3SO_3)_2$	225 (0.65 C)	2000 (6.5 C)	0.65-6.5 C
Our work	2 M $ZnSO_4$ + 0.2 M $MnSO_4$	278.5 (0.1 A/g)	600 (0.1 A/g)	0.1-2 A/g
MnOOH&MnO_2 complex[17]	1 M $ZnSO_4$ + 0.1 M $MnSO_4$	248 (0.1 A/g)	2000 (4A/g)	0.1-4 A/g
$K_{0.8}Mn_8O_{16}$ nanoparticles[18]	2 M $ZnSO_4$ + 0.1 m$MnSO_4$	300 (0.1 A/g)	1000 (1 A/g)	0.1-2 A/g
Porous MnO_x @N-C[19]	2 M $ZnSO_4$ + 0.1 M $MnSO_4$	305 (0.5 A/g)	1600 (2 A/g)	0.1-2 A/g
PANI-intercalated MnO_2[20]	2 M $ZnSO_4$ + 0.1 M $MnSO_4$	280 (0.2 A/g)	5000 (2 A /g)	0.2-3 A/g
MnO_2[21]	2 M $ZnSO_4$ + 0.2 M $MnSO_4$	290 (0.3 C)	10000 (6.5C)	0.3-6.5 C

References

1 N. Dwivedi, R. J. Yeo, N. Satyanarayana, S. Kundu, S. Tripathy, C. S. Bhatia, *Sci. Rep.* 2015, **5**, 7772.

2 C. Zhao, C. Yu, M. Zhang, H. Huang, S. Li, X. Han, Z. Liu, J. Yang, W. Xiao, J. Liang, X. Sun, J. Qiu, *Adv. Energy Mater.* 2017, **7**, 1602880.

3 A. Sumboja, C. Y. Foo, X. Wang, P. S. Lee, *Adv. Mater.* 2013, 25, 2809.

4 P. Lv, Y. Y. Feng, Y. Li, W. Feng, *J. Power Sources* 2012, **220**, 160.

5 W. Xiao, D. Hu, C. Peng, G. Z. Chen, *ACS Appl. Mater. Inter.* 2011, **3**, 3120.

6 Z.-S. Wu, W. Ren, D.-W. Wang, F. Li, B. Liu, H.-M. Cheng, *ACS Nano* 2010, **4**, 5835.

7 H. Lindström, S. Södergren, A. Solbrand, H. Rensmo, J. Hjelm, A. Hagfeldt, S.-E. Lindquist, *J. Phys. Chem. B* 1997, **101**, 7717.

8 J. Wang, J. Polleux, J. Lim, B. Dunn, *J. Phys. Chem. C* 2007, **111**, 14925.

9 Y. Fu, Q. Wei, G. Zhang, X. Wang, J. Zhang, Y. Hu, D. Wang, L. Zuin, T. Zhou, Y. Wu, S. Sun, *Adv. Energy Mater.* 2018, 8, 1801445.

10 S.-D. Han, S. Kim, D. Li, V. Petkov, H. D. Yoo, P. J. Phillips, H. Wang, J. J. Kim, K. L. More, B. Key, R. F. Klie, J. Cabana, V. R. Stamenkovic, T. T. Fister, N. M. Markovic, A. K. Burrell, S. Tepavcevic and J. T. Vaughey, *Chem. Mater.* 2017, **29**, 4874.

11 M. H. Alfaruqi, J. Gim, S. Kim, J. Song, D. T. Pham, J. Jo, Z. Xiu, V. Mathew and J. Kim, *Electrochem. Commun.* 2015, **60**, 121.

12 N. Zhang, F. Cheng, Y. Liu, Q. Zhao, K. Lei, C. Chen, X. Liu and J. Chen, *J. Am. Chem. Soc.* 2016, **138**, 12894.

13 S. Zhao, B. Han, D. Zhang, Q. Huang, L. Xiao, L. Chen, D. G. Ivey, Y. Deng and W. Wei, *J. Mater. Chem. A* 2018, **6**, 5733.

14 L. Wang, X. Cao, L. Xu, J. Chen and J. Zheng, *ACS Sustainable Chem. Eng.* 2018, **6**, 16055.

15 L. Zhao, L. Dong, W. Liu, C. Xu, *ChemistrySelect* **2018**, *3*, 12661.

16 Y. Huang, J. Liu, Q. Huang, Z. Zheng, P. Hiralal, F. Zheng, D. Ozgit, S. Su, S. Chen, P.-H. Tan, S. Zhang and H. Zhou, *NPJ Flex. Electron.* 2018, **2**, 21.

17 N. Zhang, F. Cheng, J. Liu, L. Wang, X. Long, X. Liu, F. Li and J. Chen, *Nat. Commun.* 2017, **8**, 405.

18 N. Qiu, H. Chen, Z. Yang, S. Sun and Y. Wang, *RSC Adv.* 2018, **8**, 15703.

19 G. Fang, C. Zhu, M. Chen, J. Zhou, B. Tang, X. Cao, X. Zheng, A. Pan and S. Liang, *Adv. Funct. Mater.* 2019, **29**, 1808375.

20 J. Huang, Z. Wang, M. Hou, X. Dong, Y. Liu, Y. Wang and Y. Xia, *Nat. Commun.* 2018, **9**, 2906.

21 W. Sun, F. Wang, S. Hou, C. Yang, X. Fan, Z. Ma, T. Gao, F. Han, R. Hu, M. Zhu and C. Wang, *J. Am. Chem. Soc.* 2017, **139**, 9775.